Protonic and electronic transport in hydrated thin films of the pigment eumelanin

Protonic and electronic transport in hydrated thin films of the pigment eumelanin

Julia Wünsche,[†] Yingxin Deng,[‡,⊥] Prajwal Kumar,[¶,⊥] Eduardo Di Mauro,[†] Jonathan Sayago,[†] Fabio Cicoira,[¶] Marco Rolandi,[‡] Francesca Soavi,[§] Alessandro Pezzella,[‖] and Clara Santato[*,†]

Département de Génie Physique, École Polytechnique de Montréal, C.P. 6079, Succ. Centre-ville, Montréal, Québec, Canada, H3C 3A7, Materials Science and Engineering Department, University of Washington, Seattle, WA, U.S.A., 98105, Département de Génie Chimique, École Polytechnique de Montréal, C.P. 6079, Succ. Centre-ville, Montréal, Québec, Canada, H3C 3A7, Department of Chemistry "Giacomo Ciamician" Università di Bologna, Via Selmi, 2, Bologna, Italy, 40126, and Dipartimento di Scienze Chimiche, University of Naples Federico II, Via Cintia, Complesso Monte Sant'Angelo, 21, Napoli, Italy, 80126

E-mail: clara.santato@polymtl.ca

Abstract

The electrical properties of eumelanin, a ubiquitous natural pigment, have fascinated scientists since the late 1960s. For several decades, the hydration-dependent

[*]To whom correspondence should be addressed
[†]Département de Génie Physique, École Polytechnique de Montréal
[‡]Materials Science and Engineering Department, University of Washington, Seattle
[¶]Département de Génie Chimique, École Polytechnique de Montréal
[§]Department of Chemistry "Giacomo Ciamician" Università di Bologna
[‖]Dipartimento di Scienze Chimiche, University of Naples Federico II
[⊥]These authors contributed equally to this work.

electrical properties of eumelanin have mainly been interpreted within the amorphous semiconductor model. Recent works undermined this paradigma. Here we study protonic and electronic charge carrier transport in hydrated eumelanin in thin film form. Thin films are ideal candidates for these studies since they are readily accessible to chemical and morphological characterization and potentially amenable to device applications. Current-voltage (I-V) measurements, transient current measurements with proton-transparent electrodes, and electrochemical impedance spectroscopy (EIS) measurements are reported and correlated with the results of the chemical characterization of the films, performed by X-ray photoelectron spectroscopy. We show that the electrical response of hydrated eumelanin films is dominated by ionic conduction ($10^{-4} - 10^{-3}$ S cm^{-1}), largely attributable to protons, and electrochemical processes. To propose an explanation for the electrical response of hydrated eumelanin films as observed by EIS and I-V, we considered the interplay of proton migration, redox processes, ad electronic transport. These new insights improve the current understanding of the charge carrier transport properties of eumelanin opening the possibility to assess the potential of eumelanin for organic bioelectronic applications, e.g. protonic devices and implantable electrodes, and to advance the knowledge on the functions of eumelanin in biological systems.

Introduction

Eumelanin is the most common form of the pigment melanin in the human body, with diverse functions including photoprotection, anti-oxidant behavior, metal chelation, and free radical scavenging.[1] Melanin also plays a role in melanoma skin cancer and Parkinson's disease.[2,3] Recently, biologically derived batteries and chemical sensors based on eumelanins have been reported.[4–6] Polydopamine, a melanin-like synthetic polymer, is a versatile platform for biofunctional coatings.[7]

Eumelanin is a heterogeneous macromolecule arising in part from the polymerization

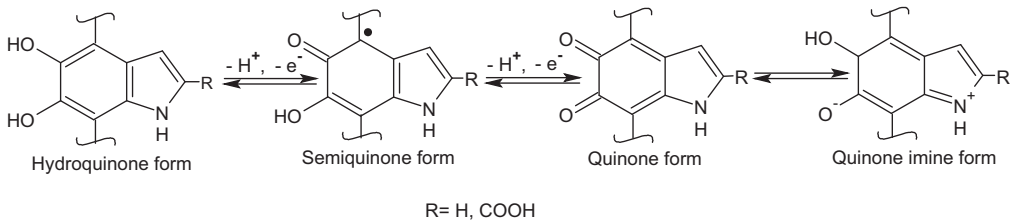

Scheme 1: Redox forms of the final monomer precursors of eumelanin (5,6-dihydroxyindole (DHI) and 5,6-dihydroxyindole-2-carboxylic acid (DHICA)). Hydroquinone (H_2Q), semiquinone (SQ), and quinone (Q) forms. The quinone imine form (QI) is the tautomer of Q.[9,16] Reversibility of the redox processes is indicated assuming that no other reactions occur after oxidation/reduction.

of L-dopa via 5,6-dihydroxyindole (DHI).[8] It is composed of oligomeric and/or polymeric species of DHI, 5,6-dihydroxyindole-2-carboxylic acid (DHICA), and their various redox forms, namely the *ortho*-hydroquinone (H_2Q), semiquinone (SQ), and (indole)quinone (Q) forms, as well as the tautomer of Q, quinone imine (QI) (Scheme 1).[8–10] From the structural point of view, eumelanins feature significant similarities with polyindole conducting polymers.[11,12] The macro- and supra-molecular structures of eumelanin depend on the (bio)-synthetic conditions.[13] Several studies indicate the formation of planar oligomer sheets, which stack via $\pi - \pi$ interaction and form disk-like aggregates.[14,15]

The electrical properties of eumelanin, characterized by a thermally activated, strongly hydration-dependent conductivity and weak photoconductivity, have fascinated scientists since the late 1960's.[17–19] Electronic band structures in analogy to inorganic semiconductors were suggested based on the strong broad-band UV-vis absorption and the π-conjugated molecular structure.[20,21] After the observation of a reversible resistive switching in eumelanin pellets reported by McGinness *et al.* in 1974,[22] electrical measurements on pellets[23–25] and thin films[26,27] have been interpreted within the amorphous semiconductor model. Within this model, the strong hydration dependence of the conductivity[28] has been explained by the increase of the dielectric constant in presence of water. This increased dielectric constant decreases the activation energy for charge carrier hopping.[17] Several reports on eumelanin pellets or thin films also present evidence of mobile protons.[18,24,27,29] However, apart from

the early work of Powell and Rosenberg based on a coulometric measurement,[18] none of these reports assigned a dominant role to protons for charge transport. Recently, Mostert *et al.* demonstrated that the amorphous semiconductor model cannot properly describe the hydration-dependent conductivity of eumelanin pellets.[30] The same authors probed the presence of locally mobile protons and extrinsic free radicals by muon spin relaxation and electron spin resonance measurements and concluded that eumelanin is a hybrid protonic-electronic conductor.[31]

We recently investigated the growth and the hydration-dependent conductivity of eumelanin thin films,[32] and the their interaction with Au electrodes.[33] It is now important to establish to which extent protons and electrons contribute to the electrical response of hydrated eumelanin in view of possible applications of eumelanin in bioelectronics. We recently investigated the growth and the hydration-dependent conductivity of eumelanin thin films,[32] and the their interaction with Au electrodes.[33] Thin films are ideal candidates for these investigations because they are readily accessible to chemical and morphological characterization and potentially amenable to device applications. Electrochemical impedance spectroscopy (EIS), current-voltage (I-V) measurements, and transient current measurements with proton-conducting contacts are reported and correlated with the chemical composition of the eumelanin thin films, investigated by X-ray photoelectron spectroscopy (XPS).

Results and discussion

Electrical characterization by EIS and I-V measurements

To characterize the electrical response of hydrated eumelanin thin films, we firstly performed an EIS survey. EIS was conducted on eumelanin films at 90% relative humidity (RH), corresponding to a water content of about (16.8 ± 0.7) wt% (Figure S1 and Table S1), with Pt electrodes in two electrode configuration (Figure 1 and S2). At zero bias, the Nyquist plot, showing the impedance Z of the sample on the complex plane, consists of a semicircle

at high frequencies (Figure 1a) and a low-frequency tail indicating ion and electron blocking electrodes (Figure 1b). This behavior is typical of electrolytes sandwiched between metal electrodes with the semicircle usually assigned to the ionic resistance in parallel to the geometric capacitance.[34,35] The blocking behavior of the electrodes dominates up to a bias of 0.2 V: the sample responds to the AC voltage by charging and discharging the double layer.

To verify that the ionic conductance associated with the semicircle can be assigned to the eumelanin bulk as opposed to currents in the water layer adsorbed on the substrate or film surface,[36] we conducted EIS measurements on eumelanin films of different thickness and on bare substrates (Figure S3). The ionic conductance was found to scale with film thickness and currents in 50 nm thick eumelanin films were on average one order of magnitude higher than on bare substrates. Eumelanin samples with electrode distances L of 10, 80, and 500 μm gave similar values for the ionic conductivity (Figure S4). We extracted an average ionic conductivity of $7.1 \cdot 10^{-4}$ S cm^{-1} with a standard deviation of $4.8 \cdot 10^{-4}$ S cm^{-1} (13 eumelanin thin film samples). Due to the high proton concentration in eumelanin, the charge carriers responsible for this conductivity are expected to be mainly protons. This is further supported by literature where the mobility of protons is reported to be at least three times larger than the mobility of other ions in hydrated polymers.[37,38] The conductivity value is comparable with the protonic conductivity of proton conducting biomaterials such as maleic chitosan,[39] proline chitosan,[40] and squid reflectin protein.[41]

With increasing bias, the onset of a second semicircle can be recognized at low frequencies in the Nyquist plots (Figure 1a and b). The diameter of this semicircle decreases when the bias is increased. This is typical of electrodes loosing their electron blocking behavior. The size of the second semicircle depends on the in-plane electrode area A (inset of Figure 1). It is smaller with respect to the first semicircle for samples with a larger A/W ratio (Figure S5 in SI), suggesting that it arises from a phenomenon at the interface, such as electrochemical reactions, rather than in the bulk. In the study of mixed conductors, the appearance of a second semicircle in the low-frequency region of the Nyquist plot and the simultaneous absence

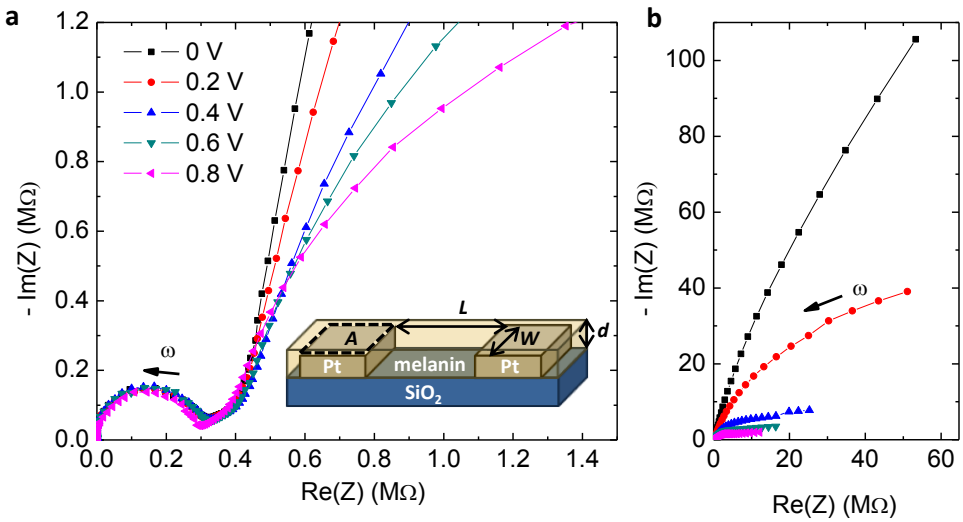

Figure 1: Nyquist plots of the EIS measurement on a eumelanin film at 90% RH, applying a bias between 0 and 0.8 V ($L = 10$ μm, $W = 24.5$ mm, $d = 50$ nm). (a) High-frequency range. The inset illustrates the sample geometry. (b) Entire frequency range ($10^{-2} - 10^{6}$ Hz).

of a capacitive low-frequency tail, in absence of electrochemical reactions, is usually taken as evidence of electronic conduction in parallel to ionic conduction.[34,42] Nevertheless, a number of charge transfer processes at the electrodes can also cause a similar low-frequency behavior, in absence of electronic conduction in the bulk. The dependence of the low-frequency semicircle on the applied bias and the in-plane electrode area indicates its electrochemical origin.

I-V characteristics of hydrated eumelanin thin films measured with the same electrode configuration (Figure 2a) also support the presence of bulk ionic conductivity and interfacial electrochemical processes. Currents at $|V| < 0.2$ V are primarily of capacitive origin, as deduced from the weak dependence on voltage and the quasi-linear dependence on the voltage sweep rate (Figure S6a in SI). A linear fit of the rate-dependence according to $I = C\frac{dV}{dt}$ yields a capacitance C of about 10^{-7} F (Figure S6b in SI). This corresponds well to typical values of the double-layer capacitance at electrode/electrolyte interfaces (10^{-5} F cm^{-2}), when taking into account not only the film cross section ($W \cdot d$), but also the in-plane electrode area ($A = 0.8$ mm^2).[43] The capacitance value is orders of magnitude higher than what is expected from dielectric polarization and is thus an indication of ionic currents in hydrated eumelanin

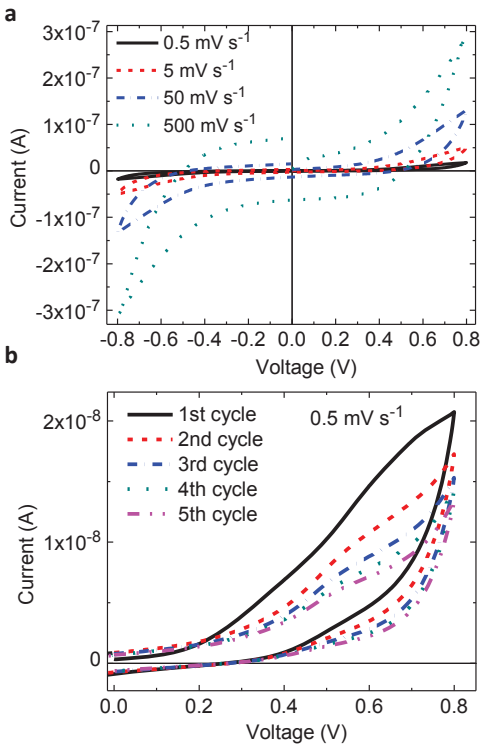

Figure 2: Current-voltage characteristics of a eumelanin film (d = 50 nm) at 90% RH, measured with coplanar Pt electrodes (L = 10 μm, W = 24.5 mm). (a) Voltage sweep rate dependence of the first cycle. (b) First five cycles of the 0.5 mV s^{-1} measurements for positive voltages.

films.[44]

At $|V| > 0.2$ V, currents show a quasi-exponential dependence on V, suggesting a non-capacitive behavior. Figure 2b shows the positive branches of the first five I-V cycles at the slowest sweep rate, 0.5 mV s^{-1}. The current decreases with each cycle and shows a broad shoulder above 0.4 V. From an electrochemical perspective, the I-V characteristics suggest the presence of irreversible redox processes at the Pt/eumelanin interfaces. The decrease of the current with each cycle is attributable to the depletion of redox species or the formation of an insulating layer at the electrode interfaces. To further investigate the importance of electrochemical reactions as compared to ionic and electronic conduction in the bulk, we investigated the scaling of the current with interelectrode distance L, film thickness d, and in-plane electrode area A (Figure S7-S9 in SI). While conduction in the bulk should scale

with the film cross section ($W \cdot d$) and increase with L^{-1}, electrochemical reactions should be more sensitive to the interface area, and thus A. Our results suggest that both transport in the bulk and processes at the electrodes determine the electrical response of the films. Interestingly, above 30 nm thickness current does not scale with film thickness any more but seems to be limited by interface processes, in line with our attribution of the current to electrochemical processes.

To shed light on possible redox processes at the electrodes, cyclic voltammetry (CV) measurements were conducted on films of *Sigma melanin*. An intense oxidation peak, located at about 0.5 V vs SCE, is observed (Figure S10 in SI). This peak has an irreversible character. CV measurements were also carried out on films with a more controlled chemical composition, using eumelanins obtained by the polymerization of DHI and DHICA (*DHI melanin* and *DHICA melanin*). Analogously to the case of *Sigma melanin*, an irreversible oxidation peak is observed during the first cycle (Figure S10 in SI).[45,46] The irreversibility of the oxidation peak likely originates from the covalent coupling (intramolecular reticulation) of the intermediate species formed at the positive electrode. Indeed, radicals and Q species formed by the oxidation of DHI moieties are reactive and may undergo coupling processes with other radicals and nucleophilic counterparts.[15,47,48] The decrease of the current density with each CV cycle can be interpreted at least in a twofold manner: polymerizing species are depleted under prolonged biasing and/or the reaction products have limited electronic conductivity. We did not observe any reversible redox activity, which is typically associated with efficient electronic conduction.

Chemical characterization by XPS

To gain insight into the molecular structure and the potential nature of charge carriers of our eumelanin samples, we performed a XPS survey. The chemical composition of eumelanin depends on its (bio-) synthetic origin and can also be affected by thin film processing.[8,32] The commercial synthetic eumelanin (*Sigma melanin*) used in this study is synthesized by

oxidation of tyrosine. The standard oxidative path leads via L-dopa to DHI and DHICA, which subsequently polymerize to eumelanin (Figure S11 in SI). Pyrrolic acids can form due to oxidative degradation. We analyzed the elemental composition and the C1s, N1s, and O1s peaks regarding the relative contribution of the various precursor units to the eumelanin macromolecule (Figure S12 and Tables S2-S4 in SI). The N1s peak suggests that a rather large portion of the units, 37%, is uncyclized. The uncyclized compounds are not detectable in the UV-Vis spectrum[49] in agreement with literature reporting strong similarities between polyphenolic and polyindolic systems.[50] The elemental ratio [C]/[N]=8.8 and the portion of C bound in -COOH moieties (8.5%), indicate a low content of pyrrolic acids. Indeed, combining these three numbers yields a composition of 22% DHI units, 41% DHICA units (both can be present in H_2Q, SQ, or Q form), 37% of L-dopa or tyrosine, and the absence of pyrrolic acids. Several impurities (F, Fe, S, Cl) were also detected in the wide scan survey. Although XPS alone does not permit to draw a complete picture of the chemical composition of *Sigma melanin*, it reveals the presence of about 0.8 -COOH moieties per monomer unit and a relatively high content of uncyclized units in the eumelanin films. Based on the XPS results, the -COOH group (pK_a 4.2[51]) should be the dominant source of protons in the eumelanin films. Further potential proton donors in eumelanin include the tautomer QI (pK_a 6.3[52]) and the hydroxyl group of SQ. However, only about one out of 1500 indole units is in SQ form at neutral pH.[52] Regardless, the high concentration of -COOH groups suggests a mayor contribution of protons to the ionic conductivity of eumelanin.[53]

Measurement of proton current using PdH_x contacts

To establish to which extent protons contribute to the electrical current in hydrated eumelanin thin films, we investigated proton transport by transient current measurements with Pd electrodes in a planar two-electrode configuration (Figure 3). Measurements were conducted at 60-80% RH, corresponding to a water content of (11.6 ± 1.0) wt% to (15.6 ± 0.2) wt% (Figure S1). PdH_x contacts have been used in the past to measure the protonic conductivity

of ice, proton conducting polymers, and biomaterials.[39–41,54,55] In its pristine state, Pd is an excellent electronic conductor and is used to measure electronic conductivity of materials. When exposed to H_2, Pd forms PdH_x, which can transfer protons between the contact and the material under investigation, according to $PdH \rightleftharpoons Pd + H^+ + e^-$. For every proton injected in the material, an electron is collected by the leads that complete the circuit. As such, PdH_x contacts are able to measure both the electronic and protonic contribution to the current in eumelanin films. For measurements at all RH (60%, 70%, and 80%) the steady-state current in eumelanin films recorded with PdH_x contacts is higher than the current measured with the Pd contacts before exposure to H_2. The difference increases with relative humidity. Thicker films of eumelanin show an enhancement of the steady-state current of up to a factor of 10 with PdH_x contacts and a very pronounced hydration dependence (Figure S13 in SI). This is an indication that the protonic component of the steady state current in melanin increases at higher RH as expected for most proton-conducting biomaterials.[39–41] From the steady-state current measured at 80% RH with PdH_x contacts, we subtract the current measured with Pd contacts at the same RH and obtain $2 \cdot 10^{-5}$ S cm^{-1} as an estimate for the proton conductivity. It has to be noted that this value is affected by factors such as contact resistance and space charge effects. Considering the difference in RH (80% for measurements with PdH_x, 90% for EIS), the value is in good agreement with the data from EIS (Figure 1) .

The transient response measured with these contacts is more difficult to interpret because it also includes a component of dielectric polarization and possibly double layer charging by ions other than protons and is limited by the small number of data points (Figure S13 in SI). Qualitatively, the difference between the transient response versus the steady state response is smaller for PdH_x contacts. This observation confirms that the increased current measured in the steady state with the PdH_x contacts arises from protons, because protons contribute to the transient response measured with Pd contacts, but should not contribute to the steady-state current.

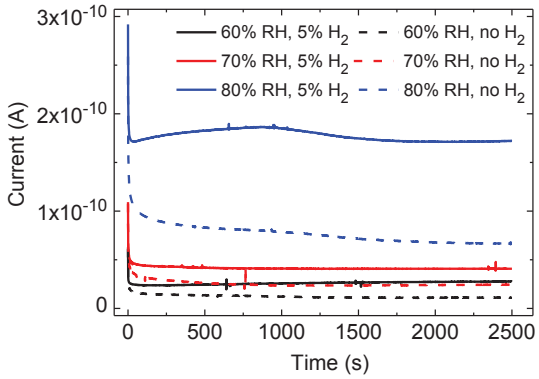

Figure 3: Transient current measurements of a eumelanin film ($d = 50$ nm) with Pd electrodes (electronic current) and PdH_x (electronic and protonic current) contacts ($L = 9$ μm, $W = 20$ μm) at 60, 70, and 80 % RH. The applied bias is 0.5 V.

Discussion on the interplay of proton migration, redox processes, and electronic transport

To understand the complex electrical response of hydrated eumelanin films as observed by EIS and I-V, the interplay of proton migration, redox processes, and electronic transport has to be considered. Before biasing, the hydrated eumelanin film contains eumelanin building blocks DHI and DHICA in different redox states (H_2Q, SQ, Q, and QI tautomer, Scheme 1) as well as protons originating from -COOH, QI, and SQ moieties, homogeneously distributed within the film (Figure 4a). -COOH groups, not explicitly shown in Figure 4, leave quasi immobile negative moieties when deprotonated. It has recently been proposed that the electronic charge carrier in eumelanin originates from the SQ free radical.[31] The density of SQ moieties is determined by the comproportionation equilibrium,[31]

$$H_2Q + Q + 2H_2O \rightleftharpoons 2\ H_3O^+ + 2\ SQ^-. \tag{1}$$

We first consider the case of low bias ($|V| < 0.2$ V), where currents are largely capacitive. Protons migrate under the influence of the external electric field and accumulate close to the negative electrode, creating a pH gradient across the film (Figure 4b). The electric field within the bulk is significantly reduced due to formation of space charges. The change in local

pH affects protonation and the comproportionation equilibrium. In aqueous suspensions of eumelanin, the SQ^- concentration increases up to a factor of 7 between pH 7 and 11.[52,56] An increase in SQ^- with pH has also been observed for hydrated pellets.[56] Thus, the density of SQ^- is expected to be higher at the positive than the negative electrode.

At higher bias ($|V| > 0.2$ V), electron transfer processes take place at the electrodes (Figure 4c). The low pH at the negative electrode should favor the reduction of Q and SQ moieties (Scheme 1).[57] The reduction of Q to SQ^- would correspond to the injection of an electron capable to contribute to electronic conduction.[31] Several processes might hinder the efficient injection. If two SQ^- are formed in close proximity, they might recombine by disproportionation to H_2Q and Q, assisted by the presence of protons (Equation 1) or undergo free-radical coupling.[58] In addition, SQ^- might be further reduced to H_2Q incorporating H^+. Species such as H^+ and O_2 could also be reduced.

At the positive electrode, the extraction of a mobile electron corresponds to the oxidation of SQ^- to Q, a process that could extend into the bulk of the film. However, tautomer formation from Q to QI followed by deprotonation of QI could limit electron transport. Furthermore, H_2Q could be oxidized to Q in a two-electron process with release of two H^+ that subsequently migrate toward the negative electrode. Irreversible processes as those discussed for CV measurements are also expected to take place.

In this picture, under sufficiently high electrical bias, an increasing number of DHI and DHICA moieties get fully reduced at the negative electrode and fully oxidized at the positive electrode. At least two processes might lead to the continuous decrease of the electronic current in eumelanin: the formation of H_2Q at the negative electrode and QI^- at the positive electrode. Both reduce the number of potential hopping sites for electrons. For a certain time, a non-capacitive current can flow even in absence of a continuous electron path between the two electrodes, the electric circuit being closed by proton migration.

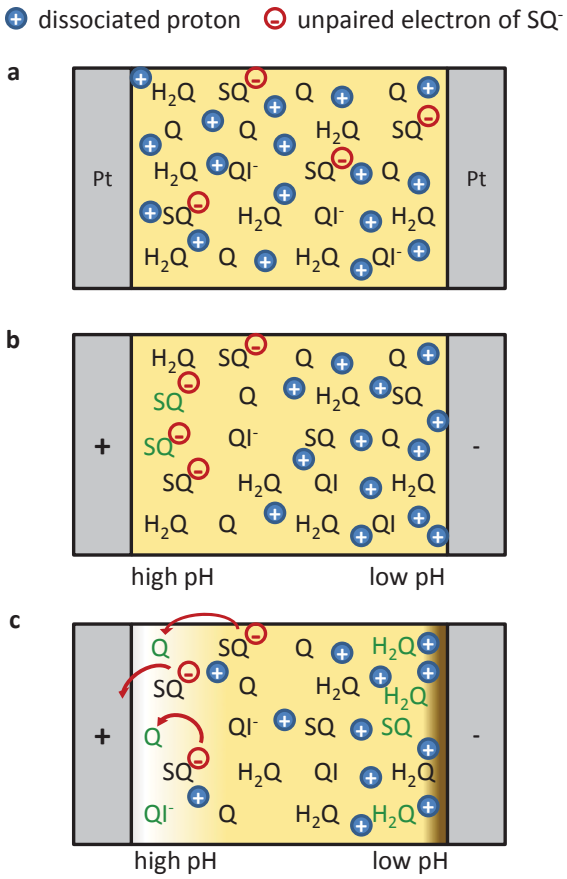

Figure 4: Illustration of the most important concepts of the model proposed for the electrical response of hydrated eumelanin films between co-planar Pt electrodes. (a) Composition of the eumelanin film before biasing including the various redox forms of DHI and DHICA (H_2Q, SQ, Q, QI tautomer). (b) Under electrical bias, proton migration affects protonation and the comproportionation equilibrium (Equation 1). (c) Possible electron transfer reactions at higher bias include the oxidation (brighter background) and reduction of eumelanin (darker background) according to Scheme 1. Moieties that changed their redox state are marked in green. While H_2Q might form an insulating layer at the negative electrode, Q provides a transport path for the electronic charge carriers.

Conclusion

In conclusion, we show that eumelanin films are proton conductive over micrometric distances and that the contribution of protons to the electrical current strongly increases with hydration. The ionic conductivity reaches about $10^{-4} - 10^{-3}$ S cm^{-1} at 90% RH, largely attributable to protons. Our results point to the importance of electrochemical reactions in the electrical response of hydrated eumelanin thin films. We propose a qualitative model to describe how the interplay of proton migration, comproportionation equilibrium, and redox processes could limit electron transport through eumelanin films. Reversible and irreversible redox processes have to be properly recognized to improve the understanding of electrical conduction in eumelanin. We are currently carrying out a systematic CV survey considering different pH and electrolyte conditions.

In perspective, two approaches can be adopted to observe electronic currents in eumelanin films. From the structural point of view, electron transport could be enabled by the use of eumelanin derived from DHI. It has recently been suggested that DHI-derived eumelanin forms planar oligomers, which assemble via π-stacking.[59] In contrast, eumelanin derived from DHICA, while leading to superior proton donating and free radical scavenging properties, forms non-planar structures.[59] The high content of -COOH and uncyclized building blocks, as detected by XPS, indicate that there might be room to improve the electronic conduction by engineering the molecular structure of eumelanin. Other H-bonded pigments, which show strong intermolecular π-stacking, have recently emerged as ambipolar semiconductors.[60,61]

Furthermore, electron and hole injection might be enhanced by the use of different electrode materials. The lack of well-defined highest occupied and lowest unoccupied molecular orbital energies for eumelanin makes a rational choice of the electrode material based on energy-level alignment difficult. In this regard, carbon nanotube electrodes, which have been shown to enhance electron and hole injection in different organic semiconductors,[62] could help to ensure that electronic currents in eumelanin are not limited by injection. In addition, a systematic cyclic voltammetry survey is being carried out on eumelanin and eu-

melanin building blocks, both in suspension and thin film forms, to locate the HOMO and LUMO levels of eumelanin.

Our results point to the need for a holistic approach, including chemical, electrochemical, and structural contributions, to uncover the charge transport properties of eumelanin films. A good understanding of these properties holds the potential to reveal bioelectronic applications of eumelanin and to advance the knowledge on the functional properties of eumelanin in biological systems.

Experimental

Sample preparation

Si/SiO_2 substrates with 50 nm thick co-planar Pt or Pd electrodes patterned by photolithography were wet-cleaned and UV-ozone treated. Eumelanin thin films were deposited from a suspension of synthetic eumelanin (Sigma Aldrich) in dimethyl sulfoxide (sonicated and filtered) by spin-coating (1 min at 1000 rpm + 30 s at 4000 rpm, 30 mg ml^{-1} suspension). Some thicker films were prepared by drop casting a diluted eumelanin suspension. Film thicknesses were determined by atomic force microscopy measurements on a scratch. Films were kept in humid air (90% relative humidity (RH)) without heating for at least 24 h before characterization for evaporation of residual solvent and hydration. The effect of residual DMSO and different thermal treatments on the electrical properties of the films is currently investigated. In measurements with Pt electrodes, two different electrode geometries were compared: an interdigitated circular design with interelectrode distance $L = 10$ μm, electrode width $W = 24.5$ mm, and total in-plane electrode area $A = 0.8$ mm^2, and a design with a straight single channel with $L = 10$ μm, $W = 4$ mm, and $A = 8$ mm^2 (see Figure 1 for definition of sample dimensions). *DHI melanin* and *DHICA melanin* used for CV measurements were obtained from DHI and DHICA by the procedure reported in Ref. 63. DHI and DHICA were prepared according to Ref. 8. Suspensions of *DHI melanin* and *DHICA*

melanin in methanol (30 mg ml^{-1}) were spin-coated on ITO substrates using a rotation speed gradient from 2000 rpm to 4000 rpm. For CV measurements, *Sigma melanin* was spin-coated on ITO substrates as described above.

Sample characterization

I-V and EIS measurements were performed in a chamber with controlled RH at 90% RH in air. The Pt electodes were contacted with micromanipulated tungsten probes. A software-controlled source/measure unit (Agilent B2902A) was used for *I-V* measurements. EIS data was acquired from 1 MHz to 0.01 Hz (10 points per decade, 50 mV oscillation amplitude) with a potentiostat (Versa STAT 4, Princeton Applied Research). The ion conductivity was evaluated from measurements on five independent samples with L=10 μm (several measurements each). For transient current measurements with proton-transparent electrodes, eumelanin was deposited on Si/SiO_2 substrates with pre-patterned Pd electrodes (L=9 μm, W=20 μm). Measurements were conducted with a semiconductor parameter analyser (Agilent 4155C) in an environmental chamber with controlled humidity under N_2 atmosphere, with and without 5% H_2. XPS measurements were taken with an ESCALAB 3 MKII from VG Scienta with a Mg Kα source. CV measurements were conducted with Versa STAT 4 (Princeton Applied Research) in 0.01 M phosphate-buffered saline solution (PBS, pH 7.4). Eumelanin films were deposited on ITO on glass, used as the working electrode (area 0.63 cm^2). A saturated calomel electrode (SCE) and a Pt foil were used as reference and counter electrode, respectively. The voltage was scanned from 0 V to positive and then to negative voltages at a rate of 50 mV s^{-1}.

Acknowledgement

The authors thank to J.-P. Lévesque, J. Bouchard, and Y. Drolet for technical support, to J. Lefebvre and S. Poulin for XPS measurements. Part of this work was carried out at the Central Facilities of École Polytechnique/Université de Montréal. J.W. is grateful to

NSERC for financial support through a Vanier Canada Graduate Scholarship and to M. Irimia-Vladu and R. Oakley for valuable discussions. C.S. acknowledges financial support by FQRNT (Equipe) and by the Québec MDEIE-PSR-SIIRI. F.C. and C.S. acknowledge financial support by NSERC (Discovery grant). F.S. acknowledges financial support by Alma Mater Studiorum-Università di Bologna under the researcher mobility program within the Italian-Canadian cooperation agreement. M.R. and Y.D. acknowledge support from the National Science Foundation Career award DMR-1150630. J.S. acknowledges financial support by CONACYT and CMC Microsystems.

Supporting Information Available

Current-voltage characteristics of eumelanin films under different conditions, transient current measurements with PdH_x electrodes on thicker films, EIS results for a different electrode geometry, XPS results and analysis, CV curves, TGA curve of hydrated eumelanin.

This material is available free of charge via the Internet at `http://pubs.acs.org/`.

Notes and References

(1) Riley, P. *Int. J. Biochem. Cell Biol.* **1997**, *29*, 1235–1239.

(2) Fedorow, H.; Tribl, F.; Halliday, G.; Gerlach, M.; Riederer, P.; Double, K. L. *Prog. Neurobiol.* **2005**, *75*, 109–124.

(3) Hill, H. Z.; Li, W.; Xin, P.; Mitchell, D. L. *Pigm. Cell Res.* **1997**, *10*, 158–161.

(4) Kim, Y. J.; Wu, W.; Chun, S.-E.; Whitacre, J. F.; Bettinger, C. J. *Proc. Natl. Acad. Sci. U. S. A.* **2013**, *110*, 20912–20917.

(5) González Orive, A.; Gimeno, Y.; Creus, A.; Grumelli, D.; Vericat, C.; Benitez, G.; Salvarezza, R. *Electrochim. Acta* **2009**, *54*, 1589–1596.

(6) Piacenti da Silva, M.; Fernandes, J. C.; de Figueiredo, N. B.; Congiu, M.; Mulato, M.; de Oliveira Graeff, C. F. *AIP Advances* **2014**, *4*, 037120.

(7) Lee, H.; Dellatore, S. M.; Miller, W. M.; Messersmith, P. B. *Science* **2007**, *318*, 426–430.

(8) D'Ischia, M.; Wakamatsu, K.; Napolitano, A.; Briganti, S.; Garcia-Borron, J.-C.; Kovacs, D.; Meredith, P.; Pezzella, A.; Picardo, M.; Sarna, T.; Simon, J. D.; Ito, S. *Pigm. Cell Melanoma R.* **2013**, *26*, 616–633.

(9) Gidanian, S.; Farmer, P. J. *J. Inorg. Biochem.* **2002**, *89*, 54–60.

(10) Pezzella, A.; Iadonisi, A.; Valerio, S.; Panzella, L.; Napolitano, A.; Adinolfi, M.; D'Ischia, M. *J. Am. Chem. Soc.* **2009**, *131*, 15270–15275.

(11) Tourillon, G.; Garnier, F. *Journal of Electroanalytical Chemistry and Interfacial Electrochemistry* **1982**, *135*, 173–178.

(12) Berkes, B. B.; Inzelt, G. *Electrochimica Acta* **2014**, *122*, 11–15.

(13) Pezzella, A.; Wünsche, J. In *Organic Electronics: Emerging Concepts and Technologies*; Cicoira, F., Santato, C., Eds.; Wiley-VCH Verlag GmbH & Co. KGaA: Weinheim, Germany, 2013.

(14) Clancy, C. M. R.; Simon, J. D. *Biochemistry* **2001**, *40*, 13353–13360.

(15) Arzillo, M.; Mangiapia, G.; Pezzella, A.; Heenan, R. K.; Radulescu, A.; Paduano, L.; D'Ischia, M. *Biomacromolecules* **2012**, *13*, 2379–2390.

(16) Díaz, P.; Gimeno, Y.; Carro, P.; González, S.; Schilardi, P. L.; Benítez, G.; Salvarezza, R. C.; Creus, A. H. *Langmuir* **2005**, *21*, 5924–5930.

(17) Rosenberg, B.; Postow, E. *Ann. N. Y. Acad. Sci.* **1969**, *158*, 158–162.

(18) Powell, M. R.; Rosenberg, B. *J. Bioenerg.* **1970**, *1*, 493–509.

(19) Potts, A. M.; Au, P. C. *Agressologie* **1968**, *9*, 225–230.

(20) Pullman, A.; Pullman, B. *Biochim. Biophys. Acta* **1961**, *54*, 384–385.

(21) Strzelecka, T. *Physiol. Chemi. Phys.* **1982**, *14*, 219–222.

(22) McGinness, J.; Corry, P.; Proctor, P. *Science* **1974**, *183*, 853–855.

(23) Jastrzebska, M.; Kocot, A.; Vij, J. K.; Zalewska-Rejdak, J.; Witecki, T. *J. Mol. Struct.* **2002**, *606*, 205–210.

(24) Gonçalves, P. J.; Filho, O. B.; Graeff, C. F. O. *J. Appl. Phys.* **2006**, *99*, 104701.

(25) Ligonzo, T.; Ambrico, M.; Augelli, V.; Perna, G.; Schiavulli, L.; Tamma, M. A.; Biagi, P. F.; Minafra, A.; Capozzi, V. *J. Non-Cryst. Solids* **2009**, *355*, 1221–1226.

(26) Abbas, M.; D'Amico, F.; Morresi, L.; Pinto, N.; Ficcadenti, M.; Natali, R.; Ottaviano, L.; Passacantando, M.; Cuccioloni, M.; Angeletti, M.; Gunnella, R. *Eur. Phys. J. E* **2009**, *28*, 285–291.

(27) Ambrico, M.; Ambrico, P. F.; Cardone, A.; Ligonzo, T.; Cicco, S. R.; Mundo, R. D.; Augelli, V.; Farinola, G. M. *Adv. Mater.* **2011**, *23*, 3332–3336.

(28) Jastrzebska, M. M.; Isotalo, H.; Paloheimo, J.; Stubb, H. *J. Biomater. Sci., Polym. Ed.* **1995**, *7*, 577–586.

(29) Bridelli, M.; Capeletti, R.; Crippa, P. *J. Electroanal. Chem.* **1981**, *128*, 555–567.

(30) Mostert, A. B.; Powell, B. J.; Gentle, I. R.; Meredith, P. *Appl. Phys. Lett.* **2012**, *100*, 093701.

(31) Mostert, A. B.; Powell, B. J.; Pratt, F. L.; Hanson, G. R.; Sarna, T.; Gentle, I. R.; Meredith, P. *Proc. Natl. Acad. Sci. U. S. A.* **2012**, *109*, 8943–8947.

(32) Wünsche, J.; Cicoira, F.; Graeff, C. F. O.; Santato, C. *J. Mater. Chem. B* **2013**, *1*, 3836–3842.

(33) Wünsche, J.; Cardenas, L.; Rosei, F.; Cicoira, F.; Gauvin, R.; Graeff, C. F. O.; Poulin, S.; Pezzella, A.; Santato, C. *Adv. Funct. Mater.* **2013**, *23*, 5591–5598.

(34) Huggins, R. A. *Ionics* **2002**, *8*, 300–313.

(35) The deviation from a vertical line at low frequencies is a general observation for solid electrolyte/electrode interfaces and reflects the non-ideal properties of the blocking interface, associated with interface roughness and ion diffusion, among others[64].

(36) Kreuer, K.-D.; Wohlfarth, A. *Angewandte Chemie (International Edition)* **2012**, *51*, 10454–10456.

(37) Stavrinidou, E.; Leleux, P.; Rajaona, H.; Khodagholy, D.; Rivnay, J.; Lindau, M.; Sanaur, S.; Malliaras, G. G. *Advanced Materials* **2013**, *25*, 4488–4493.

(38) Okada, T.; Ayato, Y. *The Journal of Physical Chemistry B* **1999**, *103*, 3315–3322.

(39) Zhong, C.; Deng, Y.; Roudsari, A. F.; Kapetanovic, A.; Anantram, M. P.; Rolandi, M. *Nat. Commun.* **2011**, *2*, 476.

(40) Deng, Y.; Josberger, E.; Jin, J.; Rousdari, A. F.; Helms, B. a.; Zhong, C.; Anantram, M. P.; Rolandi, M. *Sci. Rep.* **2013**, *3*, 2481.

(41) Ordinario, D. D.; Phan, L.; Walkup IV, W. G.; Jocson, J.-M.; Karshalev, E.; Hüsken, N.; Gorodetsky, A. A. *Nature Chemistry* **2014**, *6*, 596–602.

(42) Patel, S. N.; Javier, A. E.; Stone, G. M.; Mullin, S. a.; Balsara, N. P. *ACS Nano* **2012**, *6*, 1589–1600.

(43) Pajkossy, T.; Kolb, D. *Electrochim. Acta* **2001**, *46*, 3063–3071.

(44) For comparison, the dielectric capacitance of a parallel plate capacitor with area $A = 0.8\,\mathrm{mm}^2$, plate distance $L = 10\,\mu\mathrm{m}$, and a dielectric material with the dielectric constant of water ($\epsilon_r \approx 80$) is 10^{-10} F. The real dielectric capacitance of our samples is expected to be even much lower.

(45) Serpentini, C.-L.; Montauzon, D. D.; Comtat, M.; Ginestar, J.; Paillous, N.; Sabatier, P. *Electrochim. Acta* **2000**, *45*, 1663–1668.

(46) Tarabella, G.; Pezzella, A.; Romeo, A.; D'Angelo, P.; Coppedè, N.; Calicchio, M.; D'Ischia, M.; Mosca, R.; Iannotta, S. *J. Mater. Chem. B* **2013**, *1*, 3843–3849.

(47) Pezzella, A.; D'Ischia, M.; Napolitano, A.; Palumbo, A.; Prota, G. *Tetrahedron* **1997**, *53*, 8281–8286.

(48) Napolitano, A.; Pezzella, A.; D'Ischia, M.; Prota, G. *Tetrahedron* **1996**, *52*, 8775–8780.

(49) Wünsche, J.; Rosei, F.; Graeff, C. F. O.; Santato, C. *ECS Transactions* **2011**, *35*, 75–81.

(50) Liu, Y.; Ai, K.; Lu, L. *Chemical Reviews* **2014**, *114*, 5057–5115.

(51) Charkoudian, L. K.; Franz, K. J. *Inorg. Chem.* **2006**, *45*, 3657–3664.

(52) Szpoganicz, B.; Gidanian, S.; Kong, P.; Farmer, P. *J. Inorg. Biochem.* **2002**, *89*, 45–53.

(53) The pK_a given above have been determined in aqueous suspensions. In solid state, both pK_a and pH are unknown. Therefore, an estimation of the proton concentration from pK_a values is impossible at this stage[31].

(54) Morgan, H.; Pethig, R.; Stevens, G. T. *J. Phys. E: Sci. Instrum.* **1986**, *19*, 80–82.

(55) Josberger, E. E.; Deng, Y.; Sun, W.; Kautz, R.; Rolandi, M. *Advanced Materials* **2014**, *26*, 4986–4990.

(56) Mostert, A. B.; Hanson, G. R.; Sarna, T.; Gentle, I. R.; Powell, B. J.; Meredith, P. *J. Phys. Chem. B* **2013**, *117*, 4965–4972.

(57) Sarna, T.; Korytowski, W.; Sealy, R. *Arch. Biochem. Biophys.* **1985**, *239*, 226–233.

(58) Pezzella, A.; Crescenzi, O.; Panzella, L.; Napolitano, A.; Land, E. J.; Barone, V.; D'Ischia, M. *J. Am. Chem. Soc.* **2013**, *135*, 12142–12149.

(59) Panzella, L.; Gentile, G.; D'Errico, G.; Della Vecchia, N. F.; Errico, M. E.; Napolitano, A.; Carfagna, C.; D'Ischia, M. *Angew. Chem., Int. Ed.* **2013**, *125*, 12916–12919.

(60) Irimia-Vladu, M.; Głowacki, E. D.; Troshin, P. a.; Schwabegger, G.; Leonat, L.; Susarova, D. K.; Krystal, O.; Ullah, M.; Kanbur, Y.; Bodea, M. a.; Razumov, V. F.; Sitter, H.; Bauer, S.; Sariciftci, N. S. *Adv. Mater.* **2012**, *24*, 375–380.

(61) Głowacki, E. D.; Irimia-Vladu, M.; Kaltenbrunner, M.; Gsiorowski, J.; White, M. S.; Monkowius, U.; Romanazzi, G.; Suranna, G. P.; Mastrorilli, P.; Sekitani, T.; Bauer, S.; Someya, T.; Torsi, L.; Sariciftci, N. S. *Adv. Mater.* **2013**, *25*, 1563–1569.

(62) Valitova, I.; Amato, M.; Mahvash, F.; Cantele, G.; Maffucci, A.; Santato, C.; Martel, R.; Cicoira, F. *Nanoscale* **2013**, *5*, 4638–4646.

(63) Pezzella, A.; Barra, M.; Manini, P.; Parisi, S.; Navarra, A.; Cassinese, A.; D'Ischia, M. A. *Angew. Chem., Int. Ed.* submitted.

(64) Raistrick, I. D.; Franceschetti, D. R.; Macdonald, J. R. In *Impedance spectroscopy: theory , experiment, and applications*, 2nd ed.; Barsoukov, E., Macdonald, J. R., Eds.; John Wiley & Sons, Inc.: Hoboken, New Jersey, 2005.

Graphical TOC Entry

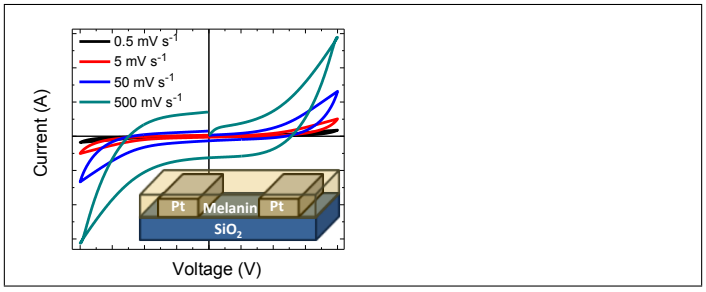

CHEMISTRY OF MATERIALS

Article

pubs.acs.org/cm

Protonic and Electronic Transport in Hydrated Thin Films of the Pigment Eumelanin

Julia Wünsche,[†] Yingxin Deng,[‡,⊥] Prajwal Kumar,[¶,⊥] Eduardo Di Mauro,[†] Erik Josberger,[#] Jonathan Sayago,[†] Alessandro Pezzella,[§] Francesca Soavi,[∥] Fabio Cicoira,[¶] Marco Rolandi,[‡] and Clara Santato*[,†]

[†]Département de Génie Physique, École Polytechnique de Montréal, C.P. 6079, Succ. Centre-ville, Montréal, Québec, Canada H3C 3A7

[‡]Materials Science and Engineering Department, University of Washington, Seattle, Washington 98105, United States

[¶]Département de Génie Chimique, École Polytechnique de Montréal, C.P. 6079, Succ. Centre-ville, Montréal, Québec, Canada H3C 3A7

[#]Electrical Engineering Department and Materials Science and Engineering Department, University of Washington, Seattle, Washington 98105, United States

[§]Dipartimento di Scienze Chimiche, University of Naples Federico II, Via Cintia, Complesso Monte Sant'Angelo, 21, Napoli, Napoli, Italy, 80126

[∥]Department of Chemistry "Giacomo Ciamician", Università di Bologna, Via Selmi, 2, Bologna, Bologna, Italy, 40126

Supporting Information

ABSTRACT: The electrical properties of eumelanin, a ubiquitous natural pigment, have fascinated scientists since the late 1960s. For several decades, the hydration-dependent electrical properties of eumelanin have mainly been interpreted within the amorphous semiconductor model. Recent works undermined this paradigm. Here we study protonic and electronic charge carrier transport in hydrated eumelanin in thin film form. Thin films are ideal candidates for these studies since they are readily accessible to chemical and morphological characterization and potentially amenable to device applications. Current−voltage (*I-V*) measurements, transient current measurements with proton-transparent electrodes, and electrochemical impedance spectroscopy (EIS) measurements are reported and correlated with the results of the chemical characterization of the films, performed by X-ray photoelectron spectroscopy. We show that the electrical response of hydrated eumelanin films is dominated by ionic conduction (10^{-4}−10^{-3} S cm^{-1}), largely attributable to protons, and electrochemical processes. To propose an explanation for the electrical response of hydrated eumelanin films as observed by EIS and *I-V*, we considered the interplay of proton migration, redox processes, and electronic transport. These new insights improve the current understanding of the charge carrier transport properties of eumelanin opening the possibility to assess the potential of eumelanin for organic bioelectronic applications, e.g. protonic devices and implantable electrodes, and to advance the knowledge on the functions of eumelanin in biological systems.

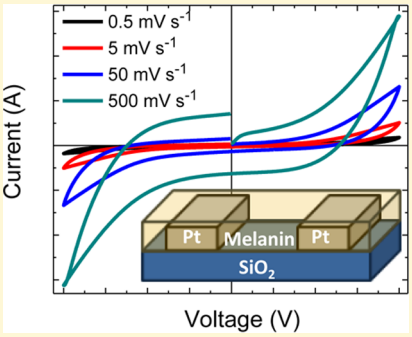

INTRODUCTION

Eumelanin is the most common form of the pigment melanin in the human body, with diverse functions including photoprotection, antioxidant behavior, metal chelation, and free radical scavenging.[1] Melanin also plays a role in melanoma skin cancer and Parkinson's disease.[2,3] Recently, biologically derived batteries and chemical sensors based on eumelanins have been reported.[4−6] Polydopamine, a melanin-like synthetic polymer, is a versatile platform for biofunctional coatings.[7]

Eumelanin is a heterogeneous macromolecule arising in part from the polymerization of L-dopa via 5,6-dihydroxyindole (DHI).[8] It is composed of oligomeric and/or polymeric species of DHI, 5,6-dihydroxyindole-2-carboxylic acid (DHICA), and their various redox forms, namely the *ortho*-hydroquinone (H_2Q), semiquinone (SQ), and (indole)quinone (Q) forms, as well as the tautomer of Q, quinone imine (QI) (Scheme 1).[8−10] From the structural point of view, eumelanins feature significant similarities with polyindole conducting polymers.[11,12] The macro- and supramolecular structures of eumelanin depend on the (bio-)synthetic conditions.[13] Several studies indicate the formation of planar oligomer sheets, which stack via π−π interaction and form disklike aggregates.[14,15]

The electrical properties of eumelanin, characterized by a thermally activated, strongly hydration-dependent conductivity, and weak photoconductivity, have fascinated scientists since the late 1960s.[17−19] Electronic band structures in analogy to

Received: August 9, 2014
Revised: December 10, 2014
Published: December 22, 2014

DOI: 10.1021/cm502939r
Chem. Mater. 2015, 27, 436−442

Scheme 1. Redox Forms of the Final Monomer Precursors of Eumelanin (5,6-Dihydroxyindole (DHI) and 5,6-Dihydroxyindole-2-carboxylic Acid (DHICA))[a]

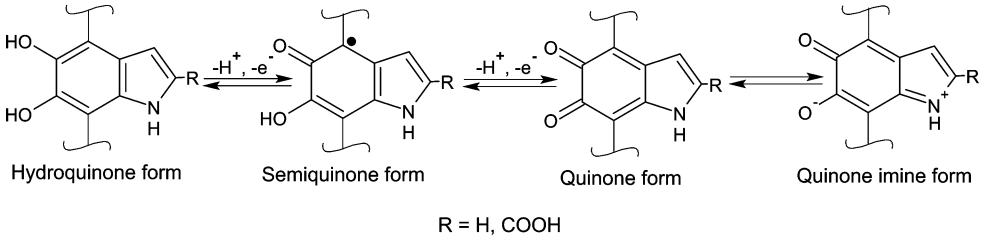

[a]Hydroquinone (H_2Q), semiquinone (SQ), and quinone (Q) forms. The quinone imine form (QI) is the tautomer of Q.[9,16] Reversibility of the redox processes is indicated assuming that no other reactions occur after oxidation/reduction.

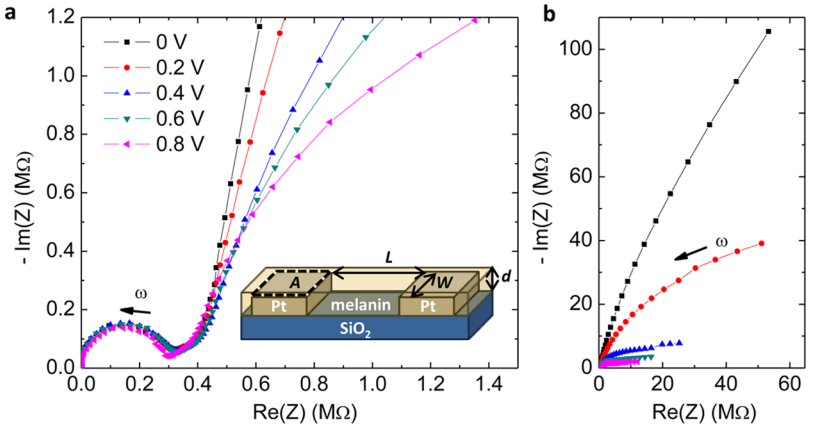

Figure 1. Nyquist plots from EIS measurements on a eumelanin film at 90% RH, applying a bias between 0 and 0.8 V (L = 10 μm, W = 24.5 mm, d = 50 nm). (a) High-frequency range. The inset illustrates the sample geometry. (b) Entire frequency range (10^{-2}–10^{6} Hz).

inorganic semiconductors were suggested based on the strong broad-band UV–vis absorption and the π-conjugated molecular structure.[20,21] After the observation of a reversible resistive switching in eumelanin pellets reported by McGinness et al. in 1974,[22] electrical measurements on pellets[23−25] and thin films[26,27] have been interpreted within the amorphous semiconductor model. Within this model, the strong hydration dependence of the conductivity[28] has been explained by the increase of the dielectric constant in the presence of water. This increased dielectric constant decreases the activation energy for charge carrier hopping.[17] Several reports on eumelanin pellets or thin films also present evidence of mobile protons.[18,24,27,29] However, apart from the early work of Powell and Rosenberg based on a coulometric measurement,[18] none of these reports assigned a dominant role to protons for charge transport. Recently, Mostert et al. demonstrated that the amorphous semiconductor model cannot properly describe the hydration-dependent conductivity of eumelanin pellets.[30] The same authors probed the presence of locally mobile protons and extrinsic free radicals by muon spin relaxation and electron spin resonance measurements and concluded that eumelanin is a hybrid protonic-electronic conductor.[31]

We recently investigated the growth and the hydration-dependent conductivity of eumelanin thin films[32] and their interaction with Au electrodes.[33] It is now important to establish to which extent protons and electrons contribute to the electrical response of hydrated eumelanin in view of possible applications of eumelanin in bioelectronics. Thin films are ideal candidates for these investigations because they are readily accessible to chemical and morphological characterization and potentially amenable to device applications. Electrochemical impedance spectroscopy (EIS), current–voltage (I-V) measurements, and transient current measurements with proton-transparent contacts are reported and correlated with the chemical composition of the eumelanin thin films, investigated by X-ray photoelectron spectroscopy (XPS).

RESULTS AND DISCUSSION

Electrical Characterization by EIS and *I-V* Measurements. To characterize the electrical response of hydrated thin films of synthetic eumelanin (Sigma-Aldrich, *Sigma melanin*), we first performed an EIS survey. EIS was conducted on eumelanin films at 90% relative humidity (RH), which corresponds to a water content in the eumelanin of about (16.8 ± 0.7) wt % (Figure S1 and Table S1 in the Supporting Information (SI)), with Pt electrodes in a two electrode configuration (Figures 1 and S2).[34] At zero bias, the Nyquist plot, showing the impedance Z of the sample on the complex plane, consists of a semicircle at high frequencies (Figure 1a) and a low-frequency tail that indicates ion and electron blocking electrodes (Figure 1b). At blocking electrodes (ideally polarizable electrodes) faradaic reactions are not taking place, and capacitive charging of the double layer is the only process occurring at the electrode/electrolyte interface. This behavior is typical of electrolytes sandwiched between metal electrodes with the semicircle usually assigned to the ionic resistance in parallel to the geometric capacitance.[35] The deviation from a vertical line at low frequencies is a general observation for solid electrolyte/electrode interfaces and reflects the nonideal properties of the blocking interface, associated with interface roughness and ion diffusion, among others.[35,36] The blocking

DOI: 10.1021/cm502939r
Chem. Mater. 2015, 27, 436−442

behavior of the electrodes dominates up to a bias of 0.2 V; the sample responds to the AC voltage by charging and discharging the double layer.

To verify that the ionic conductance associated with the semicircle can be assigned to the eumelanin bulk as opposed to currents in the water layer adsorbed on the substrate or film surface,[37] we conducted EIS measurements on eumelanin films of different thickness and on bare substrates (Figure S3). The ionic conductance scaled with film thickness and currents in 50 nm thick eumelanin films were on average 1 order of magnitude higher than on bare substrates. Eumelanin samples with electrode distances L of 10, 80, and 500 μm had similar values for the ionic conductivity (Figure S4). We extracted an average ionic conductivity of 7.1×10^{-4} S cm^{-1} with a standard deviation of 4.8×10^{-4} S cm^{-1} (13 eumelanin thin film samples). While the contribution of other ions cannot be entirely ruled out at this stage, it is conceivable to assume that the charge carriers involved in this conductivity are mainly protons. These protons would arise in melanin from the comproportionation reaction[31] and −COOH groups (see XPS data below). Furthermore, the mobility of protons in hydrated polymers is typically at least three times larger than the mobility of other ions in hydrated polymers.[38,39] The conductivity value is comparable with the protonic conductivity of proton conducting biomaterials such as maleic chitosan,[40] proline chitosan,[41] and squid reflectin protein.[42]

With increasing bias, a second semicircle onsets at low frequencies in the Nyquist plots (Figure 1a and b). The diameter of this semicircle decreases when the bias is increased. This behavior is typical of electrodes losing their electron blocking behavior. The size of the second semicircle depends on the in-plane electrode area A (inset of Figure 1) and is smaller with respect to the first semicircle for samples with a larger A/W ratio (Figure S5 in the SI). This dependence on A suggests that this semicircle arises from phenomena at the interface, such as electrochemical reactions, rather than in the bulk. In the study of mixed conductors, the appearance of a second semicircle in the low-frequency region of the Nyquist plot and the simultaneous absence of a capacitive low-frequency tail, in the absence of electrochemical reactions, is usually taken as evidence of electronic conduction in parallel to ionic conduction.[35,43] Nevertheless, a number of charge transfer processes at the electrodes can also cause a similar low-frequency behavior, in the absence of electronic conduction in the bulk. The dependence of the low-frequency semicircle on the applied bias and the in-plane electrode area indicates its electrochemical origin.

I-V characteristics of hydrated eumelanin thin films measured with the same electrode configuration (Figure 2a) also support the presence of bulk ionic conductivity and interfacial electrochemical processes. Currents at $|V| < 0.2$ V are primarily of capacitive origin, as deduced from the weak dependence on voltage and the quasi-linear dependence on the voltage sweep rate (Figure S6a in the SI). A linear fit of the rate-dependence according to $I = C((dV)/(dt))$ yields a capacitance C of about 10^{-7} F (Figure S6b in the SI). This is in good agreement with typical values of the double-layer capacitance at electrode/electrolyte interfaces (10^{-5} F cm^{-2}), when taking into account not only the film cross section ($W{\cdot}d$) but also the in-plane electrode area ($A = 0.8$ mm^2).[44] The capacitance value (10^{-7} F) is orders of magnitude higher than what is expected from dielectric polarization and is thus an indication of ionic currents in hydrated eumelanin films.[45]

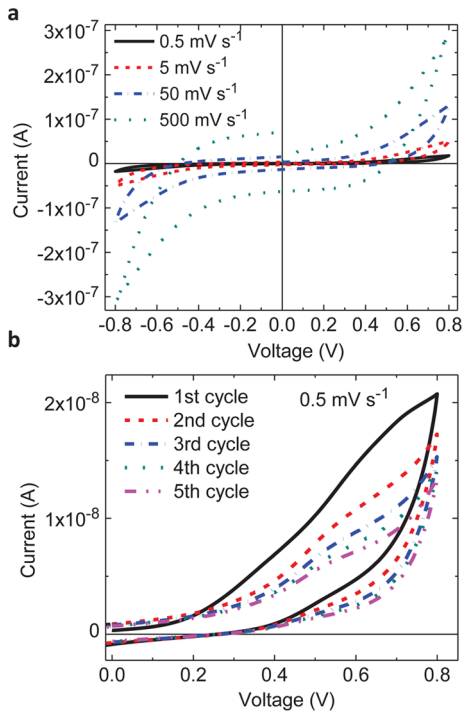

Figure 2. Current−voltage characteristics of a eumelanin film (d = 50 nm) at 90% RH, measured with coplanar Pt electrodes (L = 10 μm, W = 24.5 mm). (a) Voltage sweep rate dependence of the first cycle. (b) First five cycles of the 0.5 mV s^{-1} measurements for positive voltages.

At $|V| > 0.2$ V, currents show a quasi-exponential dependence on V, suggesting a noncapacitive behavior. Figure 2b shows the positive branches of the first five *I-V* cycles at the slowest sweep rate, 0.5 mV s^{-1}. The current decreases with each cycle with a broad shoulder above 0.4 V. From an electrochemical perspective, the *I-V* characteristics suggest the presence of irreversible redox processes at the Pt/eumelanin interfaces. The decrease of the current with each cycle is attributable to the depletion of redox species or the formation of an insulating layer at the electrode interfaces. To further investigate the importance of electrochemical reactions as compared to ionic and electronic conduction in the bulk, we investigated the scaling of the current with interelectrode distance L, film thickness d, and in-plane electrode area A (Figures S7−S9 in the SI). While conduction in the bulk should scale with the film cross section ($W{\cdot}d$) and increase with L^{-1}, electrochemical reactions should be more sensitive to the interface area and thus A. Our results suggest that both transport in the bulk and processes at the electrodes determine the electrical response of the films. Interestingly, above 30 nm thickness current does not scale with film thickness any more but seems to be limited by interface processes, in line with our attribution of the current to electrochemical processes (Figure S8).

To shed light on possible redox processes at the electrodes, cyclic voltammetry (CV) measurements were conducted on films of *Sigma melanin* in a conventional electrochemical cell. An intense oxidation peak, located at about 0.5 V vs SCE, is observed (Figure S10 in the SI). This peak has an irreversible character. CV measurements were also carried out on films with a more controlled chemical composition, using eumelanins obtained by the polymerization of DHI and DHICA (*DHI melanin* and *DHICA melanin*). Analogously to the case of *Sigma melanin*, an irreversible oxidation peak is observed during the

DOI: 10.1021/cm502939r
Chem. Mater. 2015, 27, 436−442

first cycle (Figure S10 in the SI).[46,47] The irreversibility of the oxidation peak likely originates from the covalent coupling (intramolecular reticulation) of the intermediate species formed at the positive electrode. Indeed, radicals and Q species formed by the oxidation of DHI moieties are reactive and may undergo coupling processes with other radicals and nucleophilic counterparts.[15,48,49] The decrease of the current density with each CV cycle can be interpreted at least in a 2-fold manner: polymerizing species are depleted under prolonged biasing and/or the reaction products have limited electronic conductivity. We did not observe any reversible redox activity, which is typically associated with efficient electronic conduction.

Chemical Characterization by XPS. To gain insight into the molecular structure and the potential nature of charge carriers of our eumelanin samples, we performed a XPS survey. The chemical composition of eumelanin depends on its (bio-)synthetic origin and can also be affected by thin film processing.[8,32] The commercial synthetic eumelanin (*Sigma melanin*) used in this study is synthesized by oxidation of tyrosine. The standard oxidative path leads via L-dopa to DHI and DHICA, which subsequently polymerize to eumelanin (Figure S11 in the SI). Pyrrolic acids can form due to oxidative degradation. We analyzed the elemental composition and the C 1s, N 1s, and O 1s peaks regarding the relative contribution of the various precursor units to the eumelanin macromolecule (Figure S12 and Tables S2−S4 in the SI). The N 1s peak suggests that a rather large portion of the units, 37%, is uncyclized. The uncyclized compounds are not detectable in the UV−vis spectrum[50] in agreement with literature reporting strong similarities between polyphenolic and polyindolic systems.[51] The elemental ratio [C]/[N] = 8.8, and the portion of C bound in −COOH moieties (8.5%) indicate a low content of pyrrolic acids. Indeed, combining these three numbers yields a composition of 22% DHI units, 41% DHICA units (both can be present in H_2Q, SQ, or Q form), 37% of L-dopa or tyrosine, and the absence of pyrrolic acids. Several impurities (F, Fe, S, Cl) were also detected in the wide scan survey. Although XPS alone does not permit the drawing of a complete picture of the chemical composition of *Sigma melanin*, it reveals the presence of about 0.8 −COOH moieties per monomer unit and a relatively high content of uncyclized units in the eumelanin films. Based on the XPS results, the −COOH group (pK_a 4.2[52]) should be the dominant source of protons in the eumelanin films. Further potential proton donors in eumelanin include the tautomer QI (pK_a 6.3[53]) and the hydroxyl group of SQ. However, only about one out of 1500 indole units is in the SQ form at neutral pH.[53] Regardless, the high concentration of −COOH groups suggests a major contribution of protons to the ionic conductivity of eumelanin.[54]

Measurement of Proton Current Using PdH_x Contacts. To establish to which extent protons contribute to the electrical current in hydrated eumelanin thin films, we investigated proton transport by transient current measurements with Pd and PdH_x electrodes in a planar two-electrode configuration (Figure 3).[34] Measurements were conducted at 60−80% RH, corresponding to a water content of (11.6 ± 1.0) wt % to (15.6 ± 0.2) wt % in the eumelanin thin films, respectively (Figure S1). PdH_x contacts have been used in the past to measure the protonic conductivity of ice, proton conducting polymers, and biomaterials.[40−42,55,56] In its pristine state, Pd is an excellent electronic conductor and is used to measure electronic conductivity of materials. When exposed to H_2, Pd forms

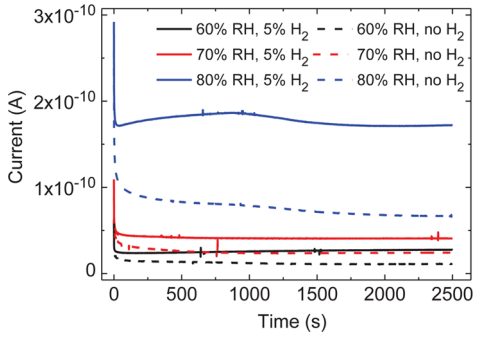

Figure 3. Transient current measurements of a eumelanin film (d = 50 nm) with Pd electrodes (electron injecting) and PdH_x (proton and electron injecting) contacts (L = 9 μm, W = 20 μm) at 60, 70, and 80% RH. The applied bias is 0.5 V.

PdH_x, which can transfer protons between the contact and the material under investigation, according to $PdH \rightleftharpoons Pd + H^+ + e^-$. For every proton injected in the material, an electron is collected by the leads that complete the circuit. As such, PdH_x contacts are able to measure both the electronic and protonic contribution to the current in eumelanin films. For measurements at all RH (60%, 70%, and 80%) the steady-state current in eumelanin films recorded with PdH_x contacts is higher than the current measured with the Pd contacts before exposure to H_2. The difference increases with relative humidity. Thicker films of eumelanin show an enhancement of the steady-state current of up to a factor of 10 with PdH_x contacts and a very pronounced hydration dependence (Figure S13 in the SI). This is an indication that the protonic component of the steady state current in melanin increases at higher RH as expected for most proton-conducting biomaterials.[40−42] From the steady-state current measured at 80% RH with PdHx contacts, we subtract the steady state current measured with Pd contacts at the same RH (80%) and obtain an estimate for the proton conductivity. This estimate is 2×10^{-5} S cm^{-1}, which is lower but comparable to the conductivity estimated from EIS (7×10^{-4} S cm^{-1}). DC measurements were performed at lower RH (80%) than EIS (90%), thus a lower protonic conductivity, which is highly hydration dependent, is expected. Additionally, other factors such as contact resistance might contribute to the lower conductivity recorded for the DC measurements compared to the EIS.

Discussion on the Interplay of Proton Migration, Redox Processes, and Electronic Transport. Our results point toward the important role of proton conduction and electrochemical processes in the complex electrical response of hydrated eumelanin films. We discuss in what follows the possible interplay between proton migration, redox processes, and electronic transport. Before biasing, the hydrated eumelanin film contains eumelanin building blocks DHI and DHICA in different redox states (H_2Q, SQ, Q, and QI tautomer, Scheme 1) as well as protons originating from −COOH, QI, and SQ moieties, homogeneously distributed within the film (Figure 4a). −COOH groups, not explicitly shown in Figure 4, leave quasi immobile negative moieties when deprotonated. It has recently been proposed that the electronic charge carrier in eumelanin originates from the SQ free radical.[31] The density of SQ moieties is determined by the comproportionation equilibrium[31]

$$H_2Q + Q + 2H_2O \rightleftharpoons 2H_3O^+ + 2SQ^- \quad (1)$$

DOI: 10.1021/cm502939r
Chem. Mater. 2015, 27, 436−442

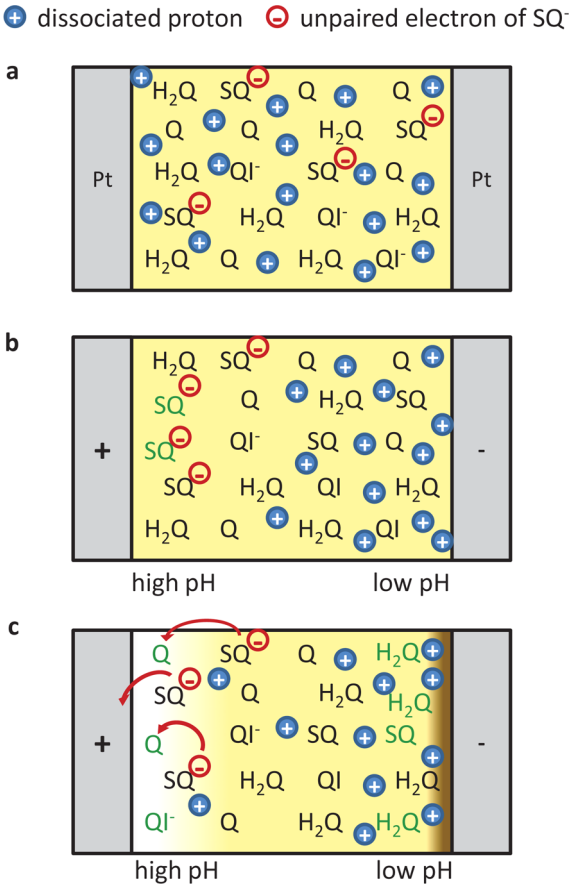

Figure 4. Illustration of the most important concepts of the model proposed for the electrical response of hydrated eumelanin films between coplanar Pt electrodes. (a) Composition of the eumelanin film before biasing including the various redox forms of DHI and DHICA (H_2Q, SQ, Q, QI tautomer). (b) Under electrical bias, proton migration affects protonation and the comproportionation equilibrium (eq 1). (c) Possible electron transfer reactions at higher bias include the oxidation (brighter background) and reduction of eumelanin (darker background) according to Scheme 1. Moieties that changed their redox state are marked in green. While H_2Q might form an insulating layer at the negative electrode, Q might provide a transport path for the electronic charge carriers.

We first consider the case of low bias ($|V| < 0.2$ V), where currents are largely capacitive. Protons migrate under the influence of the external electric field and accumulate close to the negative electrode, creating a pH gradient across the film (Figure 4b). The electric field within the bulk is significantly reduced due to formation of space charges. The change in local pH affects protonation and the comproportionation equilibrium. In aqueous suspensions of eumelanin, the SQ^- concentration increases up to a factor of 7 between pH 7 and 11.[53,57] An increase in SQ^- with pH has also been observed for hydrated pellets.[57] Thus, the density of SQ^- is expected to be higher at the positive than the negative electrode.

At higher bias ($|V| > 0.2$ V), electron transfer processes take place at the electrodes (Figure 4c). The low pH at the negative electrode should favor the reduction of Q and SQ moieties (Scheme 1).[58] The reduction of Q to SQ^- would correspond to the injection of an electron capable to contribute to electronic conduction.[31] Several processes might hinder the efficient injection. If two SQ^- are formed in close proximity, they might recombine by disproportionation to H_2Q and Q, assisted by the presence of protons (eq 1) or undergo free-radical coupling.[59] In addition, SQ^- might be further reduced to H_2Q incorporating H^+, acting as proton scavenger. Species such as H^+ and O_2 could also be reduced.

At the positive electrode, the extraction of a mobile electron corresponds to the oxidation of SQ^- to Q, a process that could extend into the bulk of the film. However, tautomer formation from Q to QI followed by deprotonation of QI to QI^- could limit electron transport. Furthermore, H_2Q could be oxidized to Q in a two-electron process with release of two H^+ that subsequently migrate toward the negative electrode. Irreversible processes as those discussed for CV measurements are also expected to take place.

In this picture, under sufficiently high electrical bias, an increasing number of DHI and DHICA moieties get fully reduced at the negative electrode and fully oxidized at the positive electrode. At least two processes might lead to the continuous decrease of the electronic current in eumelanin: the formation of H_2Q at the negative electrode and QI^- at the positive electrode. Both reduce the number of potential hopping sites for electrons. For a certain time, a noncapacitive current can flow even in the absence of a continuous electron path between the two electrodes, the electric circuit being closed by proton migration. To verify this picture and to properly identify the chemical nature of the redox species participating in the electrochemical processes, we are currently carrying out nano-IR spectroscopy and a systematic CV survey considering different pH and electrolyte conditions.

CONCLUSION

In conclusion, we show that eumelanin films are proton conductive over micrometric distances and the contribution of protons to the electrical current strongly increases with hydration. The ionic conductivity reaches about 10^{-4}–10^{-3} S cm^{-1} at 90% RH, largely attributable to protons. Our results point to the importance of electrochemical reactions in the electrical response of hydrated eumelanin thin films. We propose a qualitative model to describe how the interplay of proton migration, comproportionation equilibrium, and redox processes could limit electron transport through eumelanin films. Reversible and irreversible redox processes have to be properly recognized to improve the understanding of electrical conduction in eumelanin.

In perspective, two approaches can be adopted to observe electronic currents in eumelanin films. From the structural point of view, electron transport could be enabled by the use of eumelanin derived from DHI. It has recently been suggested that DHI-derived eumelanin forms planar oligomers, which assemble via π-stacking.[60] In contrast, eumelanin derived from DHICA, while leading to superior proton donating and free radical scavenging properties, forms nonplanar structures.[60] The high content of −COOH and uncyclized building blocks, as detected by XPS, indicate that there might be room to improve the electronic conduction by engineering the molecular structure of eumelanin. Other H-bonded pigments, which show strong intermolecular π-stacking, have recently emerged as ambipolar semiconductors.[61,62]

Furthermore, electron and hole injection might be enhanced by the use of different electrode materials. The lack of well-defined highest occupied and lowest unoccupied molecular orbital energies for eumelanin makes a rational choice of the electrode material based on energy-level alignment difficult. In this regard, carbon nanotube electrodes, which have been

DOI: 10.1021/cm502939r
Chem. Mater. 2015, 27, 436–442

shown to enhance electron and hole injection in different organic semiconductors,[63] could help to ensure that electronic currents in eumelanin are not limited by injection. In addition, a systematic cyclic voltammetry survey is being carried out on eumelanin and eumelanin building blocks, both in suspension and thin film forms, to locate the HOMO and LUMO levels of eumelanin.

Our results point to the need for a holistic approach, including chemical, electrochemical, and structural contributions, to uncover the charge transport properties of eumelanin films. A good understanding of these properties holds the potential to reveal bioelectronic applications of eumelanin and to advance the knowledge on the functional properties of eumelanin in biological systems.

EXPERIMENTAL SECTION

Sample Preparation. Si/SiO_2 substrates with 50 nm thick coplanar Pt or Pd electrodes patterned by photolithography were wet-cleaned and UV-ozone treated. Eumelanin thin films were deposited from a suspension of synthetic eumelanin (Sigma-Aldrich) in dimethyl sulfoxide (sonicated and filtered) by spin-coating (1 min at 1000 rpm +30 s at 4000 rpm, 30 mg mL^{-1} suspension). Some thicker films were prepared by drop casting a diluted eumelanin suspension. Film thicknesses were determined by atomic force microscopy measurements on a scratch. Films were kept in humid air (90% relative humidity (RH)) without heating for at least 24 h before characterization for evaporation of residual solvent and hydration. The effect of residual DMSO and different thermal treatments on the electrical properties of the films is currently investigated. In measurements with Pt electrodes, two different electrode geometries were compared: an interdigitated circular design with interelectrode distance L = 10 μm, electrode width W = 24.5 mm, and total in-plane electrode area A = 0.8 mm^2 and a design with a straight single channel with L = 10 μm, W = 4 mm, and A = 8 mm^2 (see Figure 1 for definition of sample dimensions). *DHI melanin* and *DHICA melanin* used for CV measurements were obtained from DHI and DHICA by the procedure reported in ref 64. DHI and DHICA were prepared according to ref 8. Solutions of DHI and DHICA in methanol (30 mg mL^{-1}) were spin-coated on ITO substrates using a rotation speed gradient from 2000 to 4000 rpm. For CV measurements, *Sigma melanin* was spin-coated on ITO substrates as described above.

Sample Characterization. *I-V* and EIS measurements were performed in a chamber with controlled RH at 90% RH in air. The Pt electodes were contacted with micromanipulated tungsten probes. A software-controlled source/measure unit (Agilent B2902A) was used for *I-V* measurements. EIS data was acquired from 1 MHz to 0.01 Hz (10 points per decade, 50 mV oscillation amplitude) with a potentiostat (Versa STAT 4, Princeton Applied Research). The ion conductivity was evaluated from measurements on five independent samples with L = 10 μm (several measurements each). For transient current measurements with proton-transparent electrodes, eumelanin was deposited on Si/SiO_2 substrates with prepatterned Pd electrodes (L = 9 μm, W = 20 μm). Measurements were conducted with a semiconductor parameter analyzer (Agilent 4155C) in an environmental chamber with controlled humidity under N_2 atmosphere, with and without 5% H_2. XPS measurements were taken with an ESCALAB 3 MKII from VG Scienta with a Mg Kα source. CV measurements were conducted with Versa STAT 4 (Princeton Applied Research) in 0.01 M phosphate-buffered saline solution (PBS, pH 7.4). Eumelanin films were deposited on ITO on glass, used as the working electrode (area 0.63 cm^2). A saturated calomel electrode (SCE) and a Pt foil were used as reference and counter electrode, respectively. The voltage was scanned from 0 V vs. SCE to positive and then to negative voltages at a rate of 50 mV s^{-1}.

ASSOCIATED CONTENT

Supporting Information

Current−voltage characteristics of eumelanin films under different conditions, transient current measurements with PdH_x electrodes on thicker films, EIS results for a different electrode geometry, XPS results and analysis, CV curves, TGA curve of hydrated eumelanin. This material is available free of charge via the Internet at http://pubs.acs.org.

AUTHOR INFORMATION

Corresponding Author

*E-mail: clara.santato@polymtl.ca.

Author Contributions

$^{\perp}$These authors contributed equally to this work.

Notes

The authors declare no competing financial interest.

ACKNOWLEDGMENTS

The authors thank J.-P. Lévesque, J. Bouchard, and Y. Drolet for technical support and to J. Lefebvre and S. Poulin for XPS measurements. Part of this work was carried out at the Central Facilities of École Polytechnique/Université de Montréal. J.W. is grateful to NSERC for financial support through a Vanier Canada Graduate Scholarship and to M. Irimia-Vladu, R. Oakley for valuable discussions. C.S. acknowledges financial support from FQRNT (Equipe) and from the Québec MDEIE-PSR-SIIRI. F.C. and C.S. acknowledge financial support from NSERC (Discovery grant). F.S. acknowledges financial support from Alma Mater Studiorum-Università di Bologna under the researcher mobility program within the Italian-Canadian cooperation agreement. M.R., E.J., and Y.D. acknowledge support from the National Science Foundation Career award DMR-1150630. J.S. acknowledges financial support from CONACYT and CMC Microsystems. A.P. acknowledges Italian MIUR (PRIN 2010 " 2011, 010PFLRJR PROxi project) and MC-IRSES-612538.

REFERENCES

(1) Riley, P. *Int. J. Biochem. Cell Biol.* **1997**, *29*, 1235−1239.
(2) Fedorow, H.; Tribl, F.; Halliday, G.; Gerlach, M.; Riederer, P.; Double, K. L. *Prog. Neurobiol.* **2005**, *75*, 109−124.
(3) Hill, H. Z.; Li, W.; Xin, P.; Mitchell, D. L. *Pigm. Cell Res.* **1997**, *10*, 158−161.
(4) Kim, Y. J.; Wu, W.; Chun, S.-E.; Whitacre, J. F.; Bettinger, C. J. *Proc. Natl. Acad. Sci. U. S. A.* **2013**, *110*, 20912−20917.
(5) González Orive, A.; Gimeno, Y.; Creus, A.; Grumelli, D.; Vericat, C.; Benitez, G.; Salvarezza, R. *Electrochim. Acta* **2009**, *54*, 1589−1596.
(6) Piacenti da Silva, M.; Fernandes, J. C.; de Figueiredo, N. B.; Congiu, M.; Mulato, M.; de Oliveira Graeff, C. F. *AIP Adv.* **2014**, *4*, 037120.
(7) Lee, H.; Dellatore, S. M.; Miller, W. M.; Messersmith, P. B. *Science* **2007**, *318*, 426−430.
(8) D'Ischia, M.; Wakamatsu, K.; Napolitano, A.; Briganti, S.; Garcia-Borron, J.-C.; Kovacs, D.; Meredith, P.; Pezzella, A.; Picardo, M.; Sarna, T.; Simon, J. D.; Ito, S. *Pigm. Cell Melanoma Res.* **2013**, *26*, 616−633.
(9) Gidanian, S.; Farmer, P. J. *J. Inorg. Biochem.* **2002**, *89*, 54−60.
(10) Pezzella, A.; Iadonisi, A.; Valerio, S.; Panzella, L.; Napolitano, A.; Adinolfi, M.; D'Ischia, M. *J. Am. Chem. Soc.* **2009**, *131*, 15270−15275.
(11) Tourillon, G.; Garnier, F. *J. Electroanal. Chem. Interfacial Electrochem.* **1982**, *135*, 173−178.
(12) Berkes, B. B.; Inzelt, G. *Electrochim. Acta* **2014**, *122*, 11−15.

DOI: 10.1021/cm502939r
Chem. Mater. 2015, 27, 436−442

(13) Pezzella, A.; Wünsche, J. In *Organic Electronics: Emerging Concepts and Technologies*; Cicoira, F., Santato, C., Eds.; Wiley-VCH Verlag GmbH & Co. KGaA: Weinheim, Germany, 2013.
(14) Clancy, C. M. R.; Simon, J. D. *Biochemistry* **2001**, *40*, 13353−13360.
(15) Arzillo, M.; Mangiapia, G.; Pezzella, A.; Heenan, R. K.; Radulescu, A.; Paduano, L.; D'Ischia, M. *Biomacromolecules* **2012**, *13*, 2379−2390.
(16) Díaz, P.; Gimeno, Y.; Carro, P.; González, S.; Schilardi, P. L.; Bentez, G.; Salvarezza, R. C.; Creus, A. H. *Langmuir* **2005**, *21*, 5924−5930.
(17) Rosenberg, B.; Postow, E. *Ann. N.Y. Acad. Sci.* **1969**, *158*, 158−162.
(18) Powell, M. R.; Rosenberg, B. *J. Bioenergy* **1970**, *1*, 493−509.
(19) Potts, A. M.; Au, P. C. *Agressologie* **1968**, *9*, 225−230.
(20) Pullman, A.; Pullman, B. *Biochim. Biophys. Acta* **1961**, *54*, 384−385.
(21) Strzelecka, T. *Physiol. Chemi. Phys.* **1982**, *14*, 219−222.
(22) McGinness, J.; Corry, P.; Proctor, P. *Science* **1974**, *183*, 853−855.
(23) Jastrzebska, M.; Kocot, A.; Vij, J. K.; Zalewska-Rejdak, J.; Witecki, T. *J. Mol. Struct.* **2002**, *606*, 205−210.
(24) Gonçalves, P. J.; Filho, O. B.; Graeff, C. F. O. *J. Appl. Phys.* **2006**, *99*, 104701.
(25) Ligonzo, T.; Ambrico, M.; Augelli, V.; Perna, G.; Schiavulli, L.; Tamma, M. A.; Biagi, P. F.; Minafra, A.; Capozzi, V. *J. Non-Cryst. Solids* **2009**, *355*, 1221−1226.
(26) Abbas, M.; D'Amico, F.; Morresi, L.; Pinto, N.; Ficcadenti, M.; Natali, R.; Ottaviano, L.; Passacantando, M.; Cuccioloni, M.; Angeletti, M.; Gunnella, R. *Eur. Phys. J. E* **2009**, *28*, 285−291.
(27) Ambrico, M.; Ambrico, P. F.; Cardone, A.; Ligonzo, T.; Cicco, S. R.; Mundo, R. D.; Augelli, V.; Farinola, G. M. *Adv. Mater.* **2011**, *23*, 3332−3336.
(28) Jastrzebska, M. M.; Isotalo, H.; Paloheimo, J.; Stubb, H. *J. Biomater. Sci., Polym. Ed.* **1995**, *7*, 577−586.
(29) Bridelli, M.; Capeletti, R.; Crippa, P. *J. Electroanal. Chem.* **1981**, *128*, 555−567.
(30) Mostert, A. B.; Powell, B. J.; Gentle, I. R.; Meredith, P. *Appl. Phys. Lett.* **2012**, *100*, 093701.
(31) Mostert, A. B.; Powell, B. J.; Pratt, F. L.; Hanson, G. R.; Sarna, T.; Gentle, I. R.; Meredith, P. *Proc. Natl. Acad. Sci. U. S. A.* **2012**, *109*, 8943−8947.
(32) Wünsche, J.; Cicoira, F.; Graeff, C. F. O.; Santato, C. *J. Mater. Chem. B* **2013**, *1*, 3836−3842.
(33) Wünsche, J.; Cardenas, L.; Rosei, F.; Cicoira, F.; Gauvin, R.; Graeff, C. F. O.; Poulin, S.; Pezzella, A.; Santato, C. *Adv. Funct. Mater.* **2013**, *23*, 5591−5598.
(34) It was verified that the biasing of hydrated eumelanin films with Pt or Pd electrodes at $V \leq 1$ V does not lead to dendrite formation or resistive switching as previously observed with Au electrodes.[33]
(35) Huggins, R. A. *Ionics* **2002**, *8*, 300−313.
(36) The deviation from a vertical line at low frequencies is a general observation for solid electrolyte/electrode interfaces and reflects the nonideal properties of the blocking interface, associated with interface roughness and ion diffusion, among others.[65]
(37) Kreuer, K.-D.; Wohlfarth, A. *Angew. Chem., Int. Ed.* **2012**, *51*, 10454−10456.
(38) Stavrinidou, E.; Leleux, P.; Rajaona, H.; Khodagholy, D.; Rivnay, J.; Lindau, M.; Sanaur, S.; Malliaras, G. G. *Adv. Mater.* **2013**, *25*, 4488−4493.
(39) Okada, T.; Ayato, Y. *J. Phys. Chem. B* **1999**, *103*, 3315−3322.
(40) Zhong, C.; Deng, Y.; Roudsari, A. F.; Kapetanovic, A.; Anantram, M. P.; Rolandi, M. *Nat. Commun.* **2011**, *2*, 476.
(41) Deng, Y.; Josberger, E.; Jin, J.; Rousdari, A. F.; Helms, B. A.; Zhong, C.; Anantram, M. P.; Rolandi, M. *Sci. Rep.* **2013**, *3*, 2481.
(42) Ordinario, D. D.; Phan, L.; Walkup, W. G., IV; Jocson, J.-M.; Karshalev, E.; Hüsken, N.; Gorodetsky, A. A. *Nat. Chem.* **2014**, *6*, 596−602.
(43) Patel, S. N.; Javier, A. E.; Stone, G. M.; Mullin, S. A.; Balsara, N. P. *ACS Nano* **2012**, *6*, 1589−1600.
(44) Pajkossy, T.; Kolb, D. *Electrochim. Acta* **2001**, *46*, 3063−3071.
(45) For comparison, the dielectric capacitance of a parallel plate capacitor with area $A = 0.8$ mm^2, plate distance $L = 10$ μm, and a dielectric material with the dielectric constant of water ($\varepsilon_r \approx 80$) is 10^{-10} F. The real dielectric capacitance of our samples is expected to be even much lower.
(46) Serpentini, C.-L.; Montauzon, D. D.; Comtat, M.; Ginestar, J.; Paillous, N.; Sabatier, P. *Electrochim. Acta* **2000**, *45*, 1663−1668.
(47) Tarabella, G.; Pezzella, A.; Romeo, A.; D'Angelo, P.; Coppedè, N.; Calicchio, M.; D'Ischia, M.; Mosca, R.; Iannotta, S. *J. Mater. Chem. B* **2013**, *1*, 3843−3849.
(48) Pezzella, A.; D'Ischia, M.; Napolitano, A.; Palumbo, A.; Prota, G. *Tetrahedron* **1997**, *53*, 8281−8286.
(49) Napolitano, A.; Pezzella, A.; D'Ischia, M.; Prota, G. *Tetrahedron* **1996**, *52*, 8775−8780.
(50) Wünsche, J.; Rosei, F.; Graeff, C. F. O.; Santato, C. *ECS Trans.* **2011**, *35*, 75−81.
(51) Liu, Y.; Ai, K.; Lu, L. *Chem. Rev.* **2014**, *114*, 5057−5115.
(52) Charkoudian, L. K.; Franz, K. J. *Inorg. Chem.* **2006**, *45*, 3657−3664.
(53) Szpoganicz, B.; Gidanian, S.; Kong, P.; Farmer, P. *J. Inorg. Biochem.* **2002**, *89*, 45−53.
(54) The pK_a given above have been determined in aqueous suspensions. In solid state, both pK_a and pH are unknown. Therefore, an estimation of the proton concentration from pK_a values is impossible at this stage.[31]
(55) Morgan, H.; Pethig, R.; Stevens, G. T. *J. Phys. E: Sci. Instrum.* **1986**, *19*, 80−82.
(56) Josberger, E. E.; Deng, Y.; Sun, W.; Kautz, R.; Rolandi, M. *Adv. Mater.* **2014**, *26*, 4986−4990.
(57) Mostert, A. B.; Hanson, G. R.; Sarna, T.; Gentle, I. R.; Powell, B. J.; Meredith, P. *J. Phys. Chem. B* **2013**, *117*, 4965−4972.
(58) Sarna, T.; Korytowski, W.; Sealy, R. *Arch. Biochem. Biophys.* **1985**, *239*, 226−233.
(59) Pezzella, A.; Crescenzi, O.; Panzella, L.; Napolitano, A.; Land, E. J.; Barone, V.; D'Ischia, M. *J. Am. Chem. Soc.* **2013**, *135*, 12142−12149.
(60) Panzella, L.; Gentile, G.; D'Errico, G.; Della Vecchia, N. F.; Errico, M. E.; Napolitano, A.; Carfagna, C.; D'Ischia, M. *Angew. Chem., Int. Ed.* **2013**, *125*, 12916−12919.
(61) Irimia-Vladu, M.; Głowacki, E. D.; Troshin, P. A.; Schwabegger, G.; Leonat, L.; Susarova, D. K.; Krystal, O.; Ullah, M.; Kanbur, Y.; Bodea, M. A.; Razumov, V. F.; Sitter, H.; Bauer, S.; Sariciftci, N. S. *Adv. Mater.* **2012**, *24*, 375−380.
(62) Głowacki, E. D.; Irimia-Vladu, M.; Kaltenbrunner, M.; Gsiorowski, J.; White, M. S.; Monkowius, U.; Romanazzi, G.; Suranna, G. P.; Mastrorilli, P.; Sekitani, T.; Bauer, S.; Someya, T.; Torsi, L.; Sariciftci, N. S. *Adv. Mater.* **2013**, *25*, 1563−1569.
(63) Valitova, I.; Amato, M.; Mahvash, F.; Cantele, G.; Maffucci, A.; Santato, C.; Martel, R.; Cicoira, F. *Nanoscale* **2013**, *5*, 4638−4646.
(64) Pezzella, A.; Barra, M.; Musto, A.; Navarra, A.; Alfè, M.; Manini, P.; Parisi, S.; Cassinese, A.; Criscuolo, V.; D'Ischia, M. *Mater. Horizon* **2015**, in press, DOI: 10.1039/C4MH00097H.
(65) Raistrick, I. D.; Franceschetti, D. R.; Macdonald, J. R. In *Impedance spectroscopy: theory, experiment, and applications*, 2nd ed.; Barsoukov, E., Macdonald, J. R., Eds.; John Wiley & Sons, Inc.: Hoboken, NJ, 2005.

DOI: 10.1021/cm502939r
Chem. Mater. 2015, 27, 436−442